PHYSICAL REVIEW B **106**, L041103 (2022)

Letter

Mechanical control of physical properties in the van der Waals ferromagnet $Cr_2Ge_2Te_6$ via application of electric current

Hengdi Zhao,[1] Yifei Ni,[1] Bing Hu,[1,2] Sabastian Selter,[3] Saicharan Aswartham,[3] Yu Zhang,[1]
Bernd Büchner,[3,4] Pedro Schlottmann,[5] and Gang Cao[1,*]
[1]*Department of Physics, University of Colorado at Boulder, Boulder, Colorado 80309, USA*
[2]*School of Mathematics and Physics, North China Electric Power University, Beijing 102206, China*
[3]*Institute for Solid State Research, Leibniz IFW Dresden, Helmholtzstrasse 20, 01069 Dresden, Germany*
[4]*Institute of Solid State and Materials Physics, Technische Universität Dresden, 01062 Dresden, Germany*
[5]*Department of Physics, Florida State University, Tallahassee, Florida 32306, USA*

(Received 20 January 2022; accepted 23 June 2022; published 6 July 2022)

$Cr_2Ge_2Te_6$ is a van der Waals ferromagnet with a Curie temperature at 66 K. Here we report a swift change in the magnetic ground state upon application of small DC electric current; a giant yet anisotropic magnetoelectric effect; and a sharp, lattice-driven quantum switching manifested in the *I-V* characteristic of the bulk single-crystal $Cr_2Ge_2Te_6$. At the heart of these observed phenomena is a strongly anisotropic magnetoelastic coupling that enables strongly anisotropic responses of the lattice to application of electric current and/or magnetic field, which explains the exotic phenomena in $Cr_2Ge_2Te_6$. Such a rare mechanical tunability in the magnetic semiconductors promises tantalizing prospects for unique functional materials and devices.

DOI: 10.1103/PhysRevB.106.L041103

I. INTRODUCTION

Chalcogenides as electronic materials have been studied for decades. From large thermoelectric effect, superconductivity, and photovoltaic effect to topological behavior, and most recently, novel colossal magnetoresistance (e.g., [1–4]), this class of materials is constantly surprising us with exotic phenomena. In recent years, the realization of novel physics inherent in two-dimensional (2D) semiconductors exemplified by graphene in 2004 [5] has provided impetus for a burgeoning group of studies of a large array of 2D transition-metal chalcogenides $A_2B_2X_6$ ($A =$ transition metal; $B =$ Si, Ge, or P; and $X =$ S, Se, or Te) (e.g., [6–12]). These chalcogenides commonly feature a narrow band gap (< 2 eV) and significant spin-orbit interactions. Among them is the title compound $Cr_2Ge_2Te_6$, which was first reported in 1995 [13]. It is a van der Waals ferromagnet with a Curie temperature T_C, at 66 K, which is a result of a competition between the antiferromagnetic (AFM) and ferromagnetic (FM) interactions between the $3d$ and $5p$ electrons conducting via the planar Cr-Cr pathway and the 90° interplanar Cr-Te-Cr pathway (Goodenough-Kanamori rules [14,15]), respectively [13]. The renewed interest in this and other related chalcogenides such as $Cr_2Si_2Te_6$ [6,16] arises in part from the realization of ferromagnetic order in atomic layers of these materials, such as $Cr_2Ge_2Te_6$ [7], in which the magnetic anisotropy overpowers thermal fluctuations, stabilizing the long-range magnetic order [7] (Mermin-Wagner theorem).

The magnetic anisotropy was the main motive of the most recent studies, e.g., through scanning magneto-optic Kerr microscopy (MOKE) [7], scanning tunneling spectroscopy [9], anisotropy in the magnetoresistance [10], magnetization and specific heat measurements [11], and electron spin resonance (ESR) and ferromagnetic resonance (FMR) [10,17].

Unlike transition-metal oxides where oxygen has strong electronegativity giving oxides a tendency to have ionic bonding, the chalcogenides, especially the tellurides, host instead a strong competition between metal-ligand and ligand-ligand bonding, which becomes a driver of structural and physical properties in these materials (note that the electronegativity decreases following the order of O, S, Se, and Te; the ionic bonding is no longer as significant in heavier chalcogenides) [18]. Such structural characteristics render a high susceptibility of the ground state to external stimuli that couple to the lattice. This tunability promises a rich phenomenology and indicates that the *bulk* tellurides are strongly underinvestigated as compared to other material classes.

Here we report a drastic change in the magnetic ground state upon application of a small DC electric current, a giant yet anisotropic magnetoelectric effect, and a sharp quantum switching evident in the *I-V* characteristic in the bulk single-crystal $Cr_2Ge_2Te_6$. In essence, a combination of the single-crystal x-ray diffraction as functions of both temperature and electric current with the measurements of magnetodielectric effect reveals a strong *magnetoelastic* coupling that occurs only along the a axis. Application of the electric current expands the c axis but shortens the a axis. This anisotropic change in the lattice disproportionally enhances the direct AFM exchange interaction operating via the planar Cr-Cr bond distance, thus destabilizing the precarious balance between the AFM interaction and the FM superexchange interaction via the 90° interplanar Cr-Te-Cr pathway, eventually destroying the native FM state in a critical regime of current

---

[*] gang.cao@colorado.edu

density, $0.31 < J_C < 0.55\ \mathrm{A/cm^2}$. Above J_C, a paramagnetic state emerges with a finite negative Curie-Weiss temperature, indicating a dominant AFM coupling. Accompanying these magnetic changes is a drastic reduction in the electrical resistivity by up to four orders of magnitude. Moreover, the *I-V* characteristic features a sharp quantum switching that closely tracks the lattice change in the *a* axis, offering a rare negative differential resistance. At the heart of these phenomena is the *a*-axis magnetoelastic effect in bulk $Cr_2Ge_2Te_6$, which presents tantalizing prospects for unique functional materials and devices.

Electric-current control of structural and physical properties in correlated and spin-orbit coupled materials is an emergent research topic [18]. Our recent work [19–21] indicates that electric current can effectively control quantum states in materials with a strong magnetoelastic coupling and a distorted lattice [19–21]. Note that the small DC current-controlled phenomena are fundamentally different from the Poole-Frenkel effect, which is an increase of the electrical conductivity, a consequence of a strong electric field of over 10^5 V/cm that increases the number of electrons but not their mobility [22]. In addition, studies of current-controlled phenomena require robust, innovative techniques that eliminate the effects of Joule heating. In this work, we use a small DC electric current as an external stimulus to control the structural and physical properties in $Cr_2Ge_2Te_6$.

II. EXPERIMENTAL DETAILS

Single crystals of $Cr_2Ge_2Te_6$ were grown using the self-flux technique [11]. The magnetization and electrical resistivity were simultaneously measured using a Quantum Design MPMS-XL magnetometer with a homemade probe [20]. The lattice parameters and *I-V* characteristics were also culled simultaneously using a Bruker Quest ECO single-crystal diffractometer with a home-developed capability that allows simultaneous measurements of the crystal structure and transport properties as functions of electric current and temperature [Fig. 1(a)] [19,20]. The relative permittivity was collected using a QuadTech 7600 *LCR* with a frequency range of 10 Hz–2 MHz and a Quantum Design PPMS-Dynacool with a 14 T magnet.

III. RESULTS AND DISCUSSION

$Cr_2Ge_2Te_6$ crystallizes in the rhombohedral lattice with space group *R*-3 (No. 148) [13], like its sister compound $Cr_2Si_2Te_6$ [16]. Edge-sharing $CrTe_6$ octahedra form 2D honeycomb planes. Between the planes is a van der Waals gap (∼3.35 Å, slightly smaller than 3.40 Å in $Cr_2Si_2Te_6$ [13]) [Fig. 1(a)]. A key structural element is the planar Cr-Cr bond distance *d* of two neighboring edge-sharing $CrTe_6$ octahedra, which are distorted, resulting in a discernible displacement of the Cr ions in an alternating manner, as marked by the white arrows in Fig. 1(a). The displacement is approximately along the *c* axis, facilitating the magnetic easy axis to be aligned with the *c* axis.

The lattice parameters *a* and *c* increase with increasing temperature above 140 K. As the temperature is lowered below 140 K, this trend reverses for the *a* axis but continues for the *c* axis [data in blue in Figs. 1(b) and 1(c)]. Below 140 K, the *a* axis and thus the planar Cr-Cr bond distance *d*, increase with decreasing temperature, exhibiting approximately a linear negative thermal expansion. Consequently, the increased *d* [Fig. 1(a)] weakens the direct AFM exchange interaction, facilitating the eventual occurrence of the FM state at T_C (=66 K). This behavior signals a magnetoelastic coupling along the *a* axis.

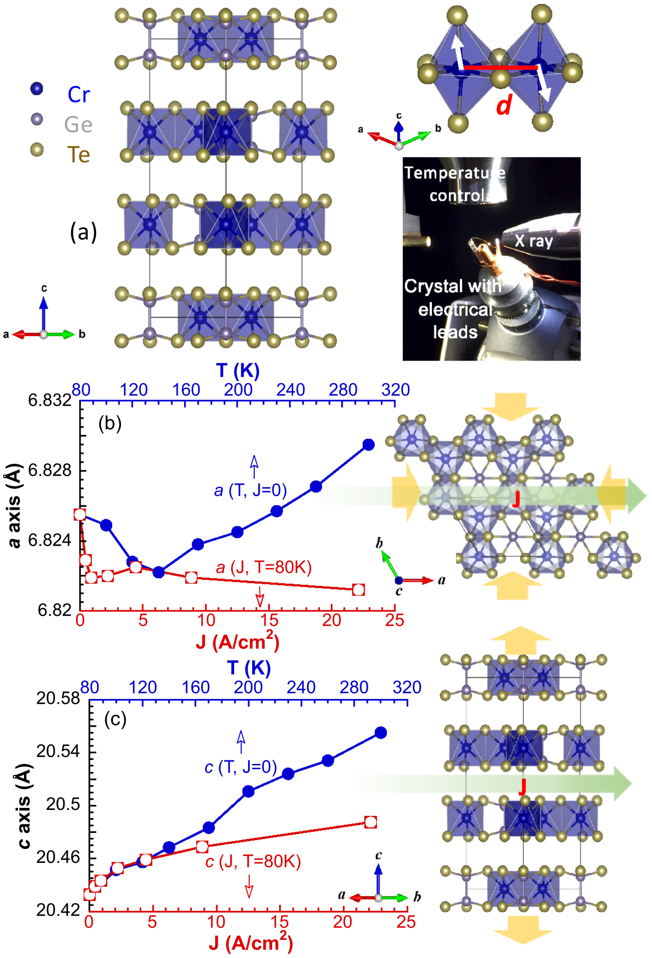

FIG. 1. Crystal structure. (a) The crystal structure of $Cr_2Ge_2Te_6$; a schematic highlighting that the Cr ions are noticeably displaced in an alternating manner, as marked by the white arrows in neighboring edge-sharing $CrTe_6$ octahedra; the Cr-Cr bond distance is denoted by *d*, which enables the direct AFM exchange interaction; a photo illustrating the home-developed setup for the simultaneous measurements of the lattice parameters and transport properties as functions of electric current and temperature. (b,c) The electric current (red) and temperature (blue) dependence of the *a* axis and *c* axis lattice parameters. The *b* axis follows the same temperature and current dependence as the *a* axis. The schematics illustrate the current-induced effect on the basal plane and the *c* axis.

The *a* and *c* axes are both susceptible to an applied electric current, but they behave in different manners. Upon the application of current, the *a* axis decreases initially and then gradually levels off with increasing current density *J* [data in red in Fig. 1(b)], whereas the *c* axis increases with increasing *J* [data in red in Fig. 1(c)]. As a result, the basal plane shrinks but the *c* axis expands [schematics in Figs. 1(b) and 1(c)]. In

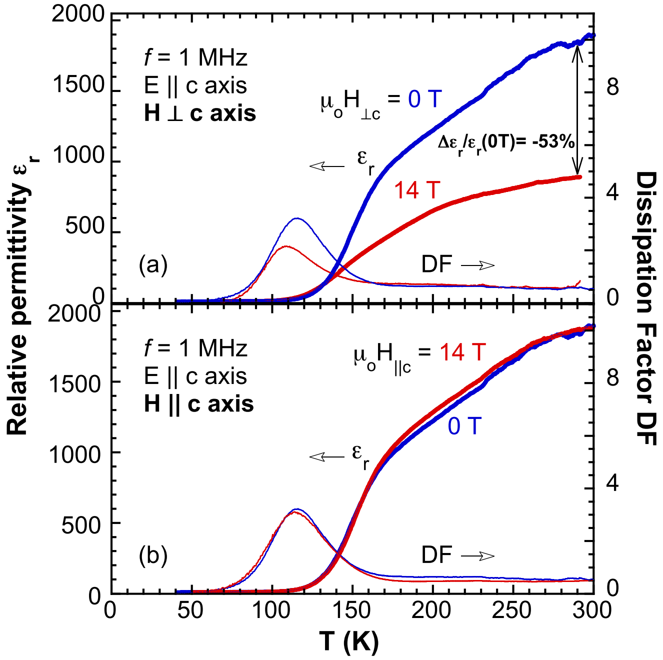

FIG. 2. Dielectric constant. The temperature dependence of the relative permittivity ε_r and the dissipation factor DF (thin lines, right scale) with the electric field E applied along the c axis and a frequency $f = 1$ MHz when (a) the magnetic field H is applied along the a axis or the magnetic hard axis and (b) H is applied along the c axis, the magnetic easy axis. Note that the magnetodielectric effect is -53% when $H||a$ and zero when $H||c$.

particular, the planar Cr-Cr bond distance d is shortened by $\sim$0.23%.

The a axis responds to $J||a$ axis and $J||c$ axis somewhat differently, especially at higher current densities $J > 10\ \mathrm{A/cm^2}$, and the Cr-Cr bond distance changes only slightly when $J||c$ axis, but the c axis responds to $J||a$ axis and $J||c$ axis almost in the same manner (see Supplemental Material [23]). Since the current-induced effects are more pronounced in a smaller $J < 10\ \mathrm{A/cm^2}$, the differences in the structural and physical properties between $J||a$ axis and $J||c$ axis are not pronounced [23]; as such, all data presented here correspond to the current applied along the a axis, which captures the essence of this work.

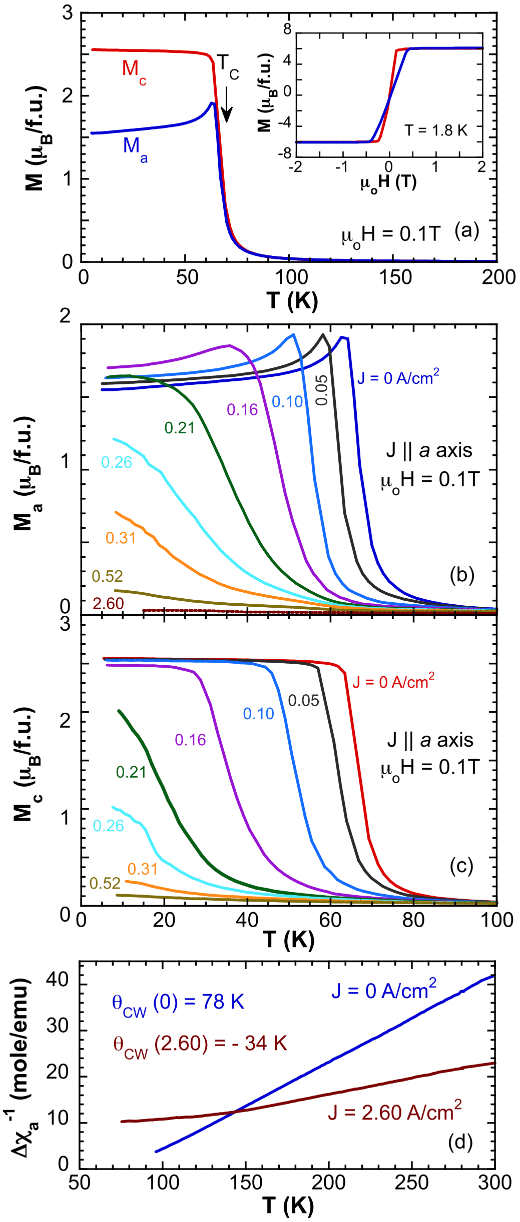

FIG. 3. Magnetic properties. The temperature dependence of (a) the a- and c-axis magnetization M_a and M_c at 0.1 T, (b) M_a with current density $J||a$, (c) M_c with $J||a$, and (d) the reciprocal magnetic susceptibility $\Delta\chi^{-1}$ ($\Delta\chi = \chi - \chi_o$, where χ_o is temperature-independent magnetic susceptibility). Inset in (a): the isothermal $M(H)$ at 1.8 K.

Before discussing the current-driven physical phenomena, let us first turn to the relative permittivity ε_r of $Cr_2Ge_2Te_6$. As shown in Fig. 2, ε_r is unusually large (up to 2500) at high temperatures (above room temperature) and decreases with decreasing temperature, eventually leveling off below 140 K, and surprisingly with no sign of the Curie-Weiss dependence, which is normally expected in dielectrics. This peculiar behavior invokes a study of the sister compound $Cr_2Si_2Te_6$ with $T_C = 33$ K [6], in which infrared spectroscopy and thermal conductivity along with complementary lattice dynamics calculations indicate that the high temperature paramagnetic phase is characterized by strong spin-lattice interactions that give rise to both glassy-behavior and a strong magnetoelastic coupling above T_C [6]. Here the large value of ε_r along with the unusual temperature dependence above 140 K manifests an extraordinarily soft lattice mode ($^2E_\mu$, infrared active) consistent with the existence of a glassy state. Note that both $Cr_2Ge_2Te_6$ and $Cr_2Si_2Te_6$ share the same crystal and magnetic structures [13]. Moreover, application of a magnetic field along the a axis or the magnetic hard axis causes a giant magnetoelectric effect, defined as $[\varepsilon_r(H) - \varepsilon_r(0\mathrm{T})]/\varepsilon_r(0\mathrm{T})$ or $\Delta\varepsilon_r/\varepsilon_r(0T)$. At $\mu_o H = 14$ T, $\Delta\varepsilon_r/\varepsilon_r(0\mathrm{T}) = -53\%$ [Fig. 2(a)]. Intriguingly, this value is essentially zero when H is applied along the c axis, the magnetic easy axis [Fig. 2(b)]. The contrasting behavior of $\Delta\varepsilon_r/\varepsilon_r(0\,\mathrm{T})$ for $H||a$ and c axis reinforces the strong a-axis magnetoelastic coupling, already evident at the aforementioned temperature and current dependence of the *a* axis [Fig. 1(b)]. With decreasing temperature, the spins are gradually locked in with an increasingly stiffened lattice via the magnetoelastic coupling, rendering the rapid reduction in ε_r below 140 K (Fig. 2) as the *a* axis starts to expand [data in blue in Fig. 1(b)], aiding the FM state to eventually emerge. The dissipation factor (DF) remains small except in the range of 90–140 K where loss becomes non-negligible (right scale in Fig. 2). Nevertheless, the soft lattice mode and the *a*-axis magnetoelastic coupling unveiled in Fig. 2 provide an important insight into the phenomena discussion below. Certainly, future infrared measurements are needed to confirm the existence of the soft lattice mode.

Now we discuss the current-controlled magnetic properties. As already established, $Cr_2Ge_2Te_6$ ferromagnetically orders at $T_C = 66$ K with an anisotropy between the *a*- and *c*-axis magnetization, M_a and M_c [Fig. 3(a)]. The peak in M_a right below T_C implies a possible canted magnetic structure within the basal plane. $Cr_2Ge_2Te_6$ hosts the Cr^{3+} ($3d^3$) ions, and the Hund's rule coupling renders a half occupation of each of the three t_{2g} orbitals, giving rise to a maximized spin state, $S = 3/2$, and an anticipated saturation moment, M_S, of 3 μ_B/Cr or 6 μ_B/f.u., which is realized at $\mu_o H = 0.16$ and 0.43 T for M_c and M_a, respectively [inset in Fig. 3(a)]. The insulating state is also a result of the half-filled t_{2g} orbitals.

Application of electric current readily suppresses T_C and the magnitude of M_a and M_c, as illustrated in Figs. 3(b) and 3(c). A Curie-Weiss analysis indicates a sign change in the Curie-Weiss temperature, θ_{CW}, from +78 K at $J = 0$ to −34 K at $J = 2.60$ A/cm^2 [Fig. 3(d)], signaling a change of the ground state. A close examination of M_a and M_c reveals a critical regime of current density of $0.31 < J_C < 0.55$ A/cm^2 (the applied currents are on the order of 10^{-5} A) above which a paramagnetic state emerges [shaded area in Figs. 4(a) and 4(b)]. The range of J_C is likely due to the magnetic anisotropy between M_a and M_c. It is revealing that these magnetic changes closely track the current-induced lattice changes in the planar Cr-Cr bond distance *d* and the *c* axis [Fig. 4(c)]. The rapidly vanishing FM state with *J* [Figs. 4(a) and 4(b)] is clearly a result of the shortened *d* that enhances the AFM interaction and the thermal fluctuations, and, to less extent, the elongated *c* axis that simultaneously weakens the FM superexchange interaction. The same notion also explains the lower T_C in $Cr_2Si_2Te_6$ (32 K) than in $Cr_2Ge_2Te_6$ (66 K). This is because $Cr_2Si_2Te_6$ has a shorter Cr-Cr bond distance *d* (3.909 Å) than that (3.934 Å) in $Cr_2Ge_2Te_6$ [13], and hence a relatively stronger AFM interaction that makes it less favorable for the FM state to stabilize at higher temperatures in $Cr_2Si_2Te_6$. Note that since the Ge or Si ions reside in each layer containing the Cr ions, the difference in the Cr-Cr bond distance must be a result of the significant difference in the ionic radius between Ge^{4+} (0.53 Å) and Si^{4+} (0.40 Å).

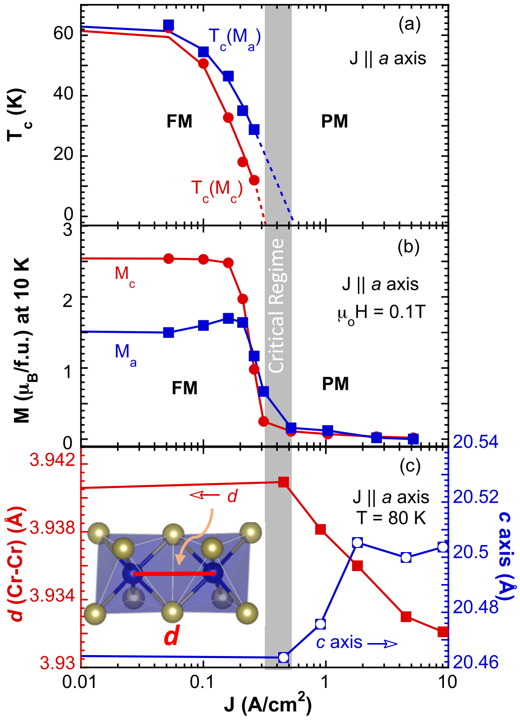

FIG. 4. Correlation between magnetic and structural properties: The current density *J* dependence of (a) the Curie temperature T_C retrieved from M_a and M_c, (b) the magnitude of M_a and M_c at 10 K, and (c) the planar Cr-Cr bond distance *d* (red) and the *c* axis (blue) at 80 K. The inset highlights *d* in the $CrTe_6$ octahedra.

The *a*-axis electrical resistivity ρ_a, which was simultaneously measured with the magnetization, decreases considerably with increasing *J*, resulting in a reduction by up to four orders of magnitude at $J = 5.2$ A/cm^2 [Fig. 5(a)]. Moreover, the *I*-*V* characteristic shows an S-shaped negative differential resistance (NDR) featuring a sharp quantum switching effect [Fig. 5(b)]. $Cr_2Ge_2Te_6$ undergoes a sharp switching to a much more metallic state from the insulating state at a threshold voltage V_{th}. Interestingly, this *I*-*V* curve (blue) closely traces the change in the *a* axis (red) at V_{th} [Fig. 5(b), inset] (note that the *I*-*V* curve and the lattice parameters were simultaneously measured). Such a lattice-driven switching effect is rare in bulk materials. The common NDR is a result of either an "electrothermal" effect or a "transferred carrier" effect [24–27], and manifests in N-shaped *I*-*V* characteristics. The S-shaped NDR is far less common but highly desirable for nonvolatile memory devices [28–30]. Previous studies indicate that so far the S-shaped NDR occurs only in a few bulk materials such as VO_2, $CuIr_2S_{4-x}Se_x$, and 1*T*-TaS_2 and is attributed to the inherent first-order structural or metal-insulator transition (e.g., [31,32]). Here the sharp switching effect that closely tracks the lattice change occurs in a material with no such first-order transition, suggesting a different mechanism. A similar behavior is also seen in spin-orbit coupled oxides such as Sr_2IrO_4 where the strong spin-orbit interaction renders a strong lattice coupling so that the *I*-*V* characteristics closely follow the current-controlled lattice change [18].

We are mindful that self-heating effects cause a continuous drift in local temperature. They are isotropic or diffusive and vary continuously with changing current [21]. Such behavior is ruled out in the present study by (i) the abrupt, simultaneous nature of the changes in T_C, *M*, and the lattice parameters (Fig. 4); (ii) the anisotropic behavior shown in Fig. 4(a) and the data in the Supplemental Material [23]; and, moreover, (iii) the current dependence of the *a* axis sharply differs from the temperature dependence of the *a* axis [data in blue in Fig. 1(b)].

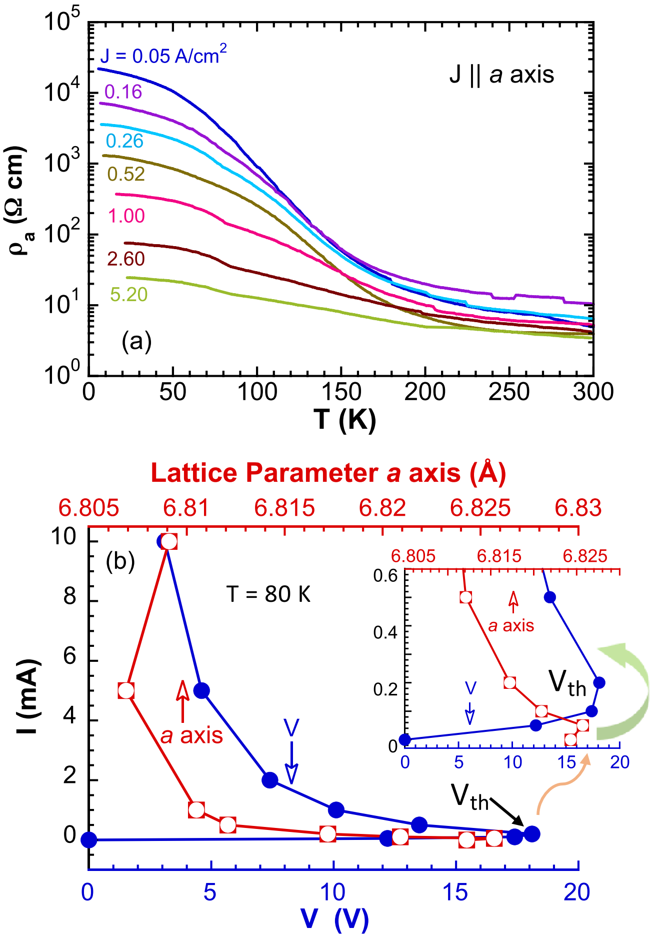

FIG. 5. Transport properties. (a) The temperature dependence of the *a*-axis resistivity ρ_a at various current density *J*. Note that ρ_a was simultaneously measured with M_a. (b) The *I*-*V* characteristic (blue) and the simultaneously measured *a* axis (red) at 80 K. The inset highlights the direct correlation between the *I*-*V* curve and the *a* axis near the switching threshold V_{th}.

IV. SUMMARY

This work demonstrates that application of small DC electric current can effectively control the structural and physical properties in the chalcogenide, and even induce phenomena seldom seen in other materials. At the heart of the tunability is the *a*-axis magnetoelastic coupling in $Cr_2Ge_2Te_6$, which has a distinct soft lattice mode at high temperatures. Our ongoing study shows strong evidence that this tunability may be widespread in other related tellurides. Empirical trends [18,21] indicate that current-controlled materials must have a ground state that is both (anti)ferromagnetic and insulating and enabled by a combined effect of Coulomb and spin-orbit interactions. Moreover, an effective current control of quantum states requires the presence of a distorted crystal structure, oftentimes, canted moments and a strong magnetoelastic coupling. With these essential ingredients, applied current is likely to be coupled with the orbitals, which in turn couple to magnetic spins via spin-orbit interactions, and the lattice via the magnetoelastic coupling. Clearly, the current-controlled phenomena in this class of materials pose tantalizing prospects for unique functional materials and devices, but a better understanding of them needs to be first established. In particular, the coupling between electric current and the lattice, orbitals, or magnetic moments in these materials has yet to be adequately described.

ACKNOWLEDGMENTS

This work is supported by the NSF via Grant No. DMR 1903888. S.A. and B.B. acknowledge the support of Deutsche Forschungsgemeinschaft (DFG) through Grant No. AS 523/4-1 and SFB 1143 (Project ID No. 247310070), respectively.

---

[1] C. B. Satterthwaite and R. Ure, Electrical and thermal properties of Bi_2Te_3, Phys. Rev. **108**, 1164 (1957).
[2] G. Snyder and E. Toberer, Complex thermoelectric materials, Nat Mater. **7**, 105 (2008).
[3] M. Z. Hasan and C. L. Kane, Colloquium: Topological insulators, Rev. Mod. Phys. **82**, 3045 (2010).
[4] Y. Ni, H. Zhao, Y. Zhang, B. Hu, I. Kimchi, and G. Cao, Colossal magnetoresistance via avoiding fully polarized magnetization in ferrimagnetic insulator $Mn_3Si_2Te_6$, Phys. Rev. B **103**, L161105 (2021).
[5] K. S. Novoselov, A. K. Geim, S. V. Morozov, D. Jiang, Y. Zhang, S. V. Dubonos, I. V. Grigorieva, and A. A. Firsov, Electric field effect in atomically thin carbon films, Science **306**, 666 (2004).
[6] L. D. Casto, A. J. Clune, M. O. Yokosuk, J. L. Musfeldt, T. J. Williams, H. L. Zhuang, M.-W. Lin, K. Xiao, R. G. Hennig, B. C. Sales *et al.*, Strong spin-lattice coupling in $CrSiTe_3$, APL Mater. **3**, 041515 (2015).
[7] C. Gong, L. Li, Z. Li, H. Ji, A. Stern, Y. Xia, T. Cao, W. Bao, C. Wang, Y. Wang *et al.*, Discovery of intrinsic ferromagnetism in two-dimensional van der Waals crystals, Nature (London) **546**, 265 (2017).
[8] H. Ji, R. A. Stokes, L. D. Alegria, E. C. Blomberg, M. A. Tanatar, A. Reijnders, L. M. Schoop, T. Liang, R. Prozorov, K. S. Burch *et al.*, A ferromagnetic insulating substrate for the epitaxial growth of topological insulators, J. Appl. Phys. **114**, 114907 (2013).
[9] Z. Hao, H. Li, S. Zhang, X. Li, G. Lin, X. Luo, Y. Sun, Z. Liu, and Y. Wang, Atomic scale electronic structure of the ferromagnetic semiconductor $Cr_2Ge_2Te_6$, Sci. Bull. **63**, 825 (2018).
[10] W. Liu, Y. Wang, Y. Han, W. Tong, J. Fan, L. Pi, N. Hao, L. Zhang, and Y. Zhang, Anisotropic magnetoresistance behaviors in the layered ferromagnetic $Cr_2Ge_2Te_6$, J. Phys. D: Appl. Phys. **53**, 025101 (2020).
[11] S. Selter, G. Bastien, A. U. B. Wolter, S. Aswartham, and B. Büchner, Magnetic anisotropy and low-field magnetic phase

diagram of the quasi-two-dimensional ferromagnet $Cr_2Ge_2Te_6$, Phys. Rev. B **101**, 014440 (2020).

[12] A. Devarakonda, H. Inoue, S. Fang, C. Ozsoy-Keskinbora, T. Suzuki, M. Kriener, L. Fu, E. Kaxiras, D. C. Bell, and J. G. Checkelsky, Clean 2D superconductivity in a bulk van der Waals superlattice, Science **370**, 231 (2020).

[13] V. Carteauxts, D. Brunet, G. Ouvrard, and G. André, Crystallographic, magnetic, and electronic structures of a new layered ferromagnetic compound $Cr_2Ge_2Te_6$, J. Phys: Condens. Matter **7**, 69 (1995).

[14] J. B. Goodenough, Theory of the role of covalence in the perovskite-type manganites [La, M(II)]MnO_3, Phys. Rev. **100**, 564 (1955).

[15] J. Kanamori, Superexchange interaction and symmetry properties of electron orbitals, J. Phys. Chem. Solids **10**, 87 (1959).

[16] V. Carteaux, G. Ouvrard, J. C. Grenier, and Y. Laligant, Magnetic structure of the new layered ferromagnetic chromium hexatellurosilicate $Cr_2Si_2Te_6$, J. Magn. Magn. Mater. **94**, 127 (1991).

[17] J. Zeisner, A. Alfonsov, S. Selter, S. Aswartham, M. P. Ghimire, M. Richter, J. van den Brink, B. Büchner, and V. Kataev, Magnetic anisotropy and spin-polarized two-dimensional electron gas in the van der Waals ferromagnet $Cr_2Ge_2Te_6$, Phys. Rev. B **99**, 165109 (2019).

[18] G. Cao and L. E. De Long, *Physics of Spin-Orbit-Coupled Oxides* (Oxford University Press, Oxford, 2021).

[19] G. Cao, J. Terzic, H. D. Zhao, H. Zheng, L. E. De Long, and P. Riseborough, Electrical Control of Structural and Physical Properties via Strong Spin-Orbit Interactions in Sr_2IrO_4, Phys. Rev. Lett. **120**, 017201 (2018).

[20] H. Zhao, B. Hu, F. Ye, C. Hoffmann, I. Kimchi, and G. Cao, Nonequilibrium orbital transitions via applied electrical current in calcium ruthenates, Phys. Rev. B **100**, 241104(R) (2019).

[21] G. Cao, Topical review: Towards electrical-current control of quantum states in spin-orbit-coupled matter, J. Phys.: Condens. Matter **32**, 423001 (2020).

[22] J. Frenkel, On pre-breakdown phenomena in insulators and electronic semi-conductors, Phys. Rev. **54**, 647 (1938).

[23] See Supplemental Material at http://link.aps.org/supplemental/10.1103/PhysRevB.106.L041103 for additional experimental data.

[24] T. K. Higman, L. M. Miller, M. E. Favaro, M. A. Emanuel, K. Hess, and J. J. Coleman, Room-temperature switching and negative differential resistance in the heterostructure hot-electron diode, Appl. Phys. Lett. **53**, 1623 (1988).

[25] F. A. Chudnovskii, A. L. Pergament, G. B. Stefanovich, P. Somasundaram, and J. M. Honig, Electronic switching in $CuIr_2S_{4-x}Se_x$, Phys. Status Solidi A **162**, 601 (1997).

[26] A. L. Pergament, G. Stefanovich, A. Velichko, and S. D. Khanin, Electronic switching and metal-insulator transitions in compounds of transition metals, in *Condensed Matter at the Leading Edge*, edited by M. P. Das (Nova Science Publishers, Hauppauge, NY, 2006), Chap. 1, pp. 1–67.

[27] F. A. Chudnovskii, L. L. Odynets, A. L. Pergament, and G. B. Stefanovich, Electroforming and switching in oxides of transition metals: The role of metal–insulator transition in the switching mechanism, J. Solid State Chem. **122**, 95 (1996).

[28] D S Jeong, R. Thomas, R. S. Katiyar, J. F. Scott, H. Kohlstedt, A. Petraru, and C. S. Hwang, Emerging memories: Resistive switching mechanisms and current status, Rep. Prog. Phys. **75**, 076502 (2012).

[29] G. I. Meijer, Who wins the nonvolatile memory race? Science **319**, 1625 (2008).

[30] K. Saha, R. Nandkishore, and S. A. Parameswaran, Valley-selective Landau-Zener oscillations in semi-Dirac p-n junctions, Phys. Rev. B **96**, 045424 (2017).

[31] A. W. Tsen, R. Hovden, D. Wang, Y. D. Kim, J. Okamoto, K. A. Spoth, Y. Liu, W. Lu, Y. Sun, J. C. Hone, L. F. Kourkoutis, P. Kim, and A. N. Pasupathy, Structure and control of charge density waves in two-dimensional $1T$-TaS_2, Proc. Natl. Acad. Sci. USA **112**, 15054 (2015).

[32] K. Okimura, N. Ezreena, Y. Sasakawa, and J. Sakai, Electric-field-induced multistep resistance switching in planar VO_2/c-Al_2O_3 structure, Jpn. J. Appl. Phys. **48**, 065003 (2009).